Journal of Physics: Conference Series **689** (2016) 012021 doi:10.1088/1742-6596/689/1/012021

Measurement of cosmogenic radioactive products in xenon and copper

Francesco Piastra[1]

[1]Department of Physics, University of Zürich, Winterthurerstrasse 190, CH-8057, Zürich, Switzerland

E-mail: `fpiastra@physik.uzh.ch`

Abstract. Rare events searches, such as direct dark matter detection or neutrinoless double beta decay ($0\nu\beta\beta$) observation, using liquid xenon as target and detection medium require ultra-low background to fully exploit the physics potential. Cosmogenic activation of the detector components, and even more importantly, of the xenon itself might have undesired impact on the background and the final sensitivity of the experiment. Since no measurement of cosmogenic activation of xenon was present in literature so far, we performed such a measurement exposing of a natural xenon sample to the cosmic radiation at the Jungfraujoch research station at an altitude of 3470 m above sea level for 245 days. This study was complemented with a ultra pure copper sample that was activated together with the xenon. We directly observed, with gamma-ray spectrometry, the production of ^{7}Be, ^{101}Rh, ^{125}Sb, ^{126}I and ^{127}Xe in xenon, out of which only ^{125}Sb could potentially lead to a background relevant for multi-ton scale direct dark matter search. The production rates for five out of eight radioactive isotopes in copper are in good agreement with the only dedicated measurement present in literature. The production rates measured for both samples were compared with the predictions obtained with commonly used software packages. The latter showed a systematic under-estimation, especially for xenon.

1. Introduction

Particle detection based on liquid Xe (LXe) was widely developed in the last decade mainly in view of direct dark matter searches [1–5].

The expected spectrum of nuclear recoils from the elastic scattering of a weakly interacting massive particle (WIMP) off a nucleus has a quasi-exponential shape [6, 7]. Hence, the low energy threshold of such an experiment can heavily affect the detection sensitivity, especially for low mass WIMPs ($\lesssim$ GeV/c^2). Among the particle detection media, LXe features one of the highest scintillation and ionization yield [8, 9] making this material one of the best candidates for dark matter searches.

Background from radioactive isotopes (radiogenic) and from cosmic rays (cosmogenic) may severely limit the detection sensitivity of any experiment searching for rare events. The former are present as residuals in every detector's materials or dissolved in the LXe itself (intrinsic sources), while the latter can be suppressed only operating the detector in deep underground laboratories, where the nuclear component of the cosmic rays (CR) is absent and the muonic component is suppressed by several orders of magnitude. The relatively high atomic number (Z=54) and density ($\rho \simeq 2.9\,\mathrm{g/cm^3}$) of LXe provide a good self-shielding power to γ and β rays able to efficiently suppress the radiogenic background in the most internal regions of the detec-

Table 1. Potential double β emitters of natural xenon. The half-lives of the double-beta decay isotopes ^{124}Xe, ^{134}Xe and ^{136}Xe are from the NuDat 2.6 database [16], the range for the double electron capture isotope ^{126}Xe is a theoretical prediction from [17]. The natural isotopic abundances are from [18].

Xe mass number	124	126	134	136
Abundance [%]	0.09(1)	0.09(1)	10.44(10)	8.87(16)
$T_{1/2}$ [yr]	$>1.6\times10^{14}$	$[5\text{-}12]\times10^{25}$	$>5.8\times10^{22}$	2.165×10^{21}

tor's sensitive volume. However this is not anymore true for intrinsic backgrounds such as ^{85}Kr and ^{222}Rn, that must be reduced to few ppt and few μBq, respectively. Moreover natural Xe has only few very long-lived isotopes that decay with double beta mechanism, listed in Table 1. Out of the potential double beta emitters, listed in Table 1, only the ^{136}Xe was observed so far and is currently used as source isotope for $0\nu\beta\beta$ searches [12–15].

The next generation ton and multi-ton scale LXe based detectors, in construction or in design phase, aim to probe the WIMP-nucleon spin independent cross section to few $\times10^{-47}\,\mathrm{cm}^2$ [4] with $\sim 2\,\mathrm{yr}\times$ ton of exposure or even to few $\times10^{-48}\,\mathrm{cm}^2$ [10, 11] with $\sim 20\,\mathrm{yr}\times$ ton. For the next-to-next multi-ton scale detectors, already in advanced design phase [5], the goal is to be sensitive to the ultimate cross section of $\sim 2\times10^{-49}\,\mathrm{cm}^2$ (with exposures of $\sim 10^2\,\mathrm{yr}\times$ ton), where the coherent neutrino-nucleus scattering events, which produce the same kind of signals expected from WIMP scatters off nuclei, become the dominant irreducible background. In detectors with these mass scales the radiogenic γ and β backgrounds will be dominated by intrinsic sources as detailed in [5]. The Xe exposure to the CR, during the production, transportation and storage above ground might produce unstable long lived nuclei which could result in an additional intrinsic source of background. Hence, it is critical, in particular for the next generations dark matter search experiments, to be able to predict the Xe cosmogenic activation and understand the maximum tolerable exposure to the cosmic rays (CR).

Software packages, like ACTIVIA [19] and COSMO [20], are able to predict the activation of yield of various materials given their isotopic composition, the nuclear CR spectrum and the exposure time. Calculations of Xe cosmogenic activation were performed with both codes for the XENON100 experiment [1] and resulted in large tension with the measured background [21, 22]. The main cause of the discrepancy was attributed to the lack of knowledge of the production cross sections of Xe, which are implemented in the codes using semi-empirical models developed by Silberberg and Tsao [23–25].

Here we report the first dedicated study of cosmogenic activation of Xe, recently published in [26], where a 2.04 kg research-grade xenon (impurities <10 ppm) with natural isotopic aboundances was exposed to cosmic rays for 245 day at an altitude of 3450 m at the "High Altitude Research Station Jungfraujoch" [27]. A 10.35 kg oxigen-free high conductivity (OFHC) copper sample was activated together with the xenon in order to provide a benchmark for our activation measurements and predictions. This sample came from the same high pure copper batch (impurities <100 ppm) used to build inner components of the XENON100 detector (sample 6 of Table 1 in [28]).

2. Measurement and analysis of the activated samples

Before the exposure the xenon was stored underground for more than 1.5 yr at the Laboratori Nazionali del Gran Sasso (LNGS, Italy), where we assume that no activation takes place. The xenon sample was contained in a 1 liter stainless steel bottle ($m = 2.9\,\mathrm{kg}$) at a pressure of $\sim 100\,\mathrm{bar}$ ($\overline{T} \sim 20\,°\mathrm{C}$). In order to avoid the measurement results being dominated by the activation of the stainless steel bottle we used two identical bottles, one always kept underground and used for the γ measurements and the other used to expose the xenon to the CR. The gas transfer between the bottles was performed in the underground laboratory before and after the activation.

The nuclear activation processes in atmosphere are dominated by the high-energy nucleons, while the atmospheric muons play only a sub-dominant role because of their lower flux [29] and their smaller cross section [30, 31]. In order to compare our measurements with the predictions from the software packages, the activation values at high-altitude must be converted to sea level production rates. For our calculations we used the CR spectrum taken from [32, 33] (sea level values) scaled for the atmospheric depth according to [34]. The atmospheric depth at the activation site was determined by the use of the U.S. Standard Atmosphere 1976 model [35].

For both the samples, before and after the activation, γ spectra were acquired with the high purity germanium detector Gator [36], running at the LNGS underground laboratory. The background of this spectrometer is $< 0.1\,\mathrm{counts{\cdot}day^{-1}keV^{-1}}$ over the entire energy region (from 50 to 2700 keV), and is sensitive to the contaminations of the most common γ emitters. The γ spectra of the xenon sample are shown in Figure 1 with the positions of the most relevant lines of the detected radioisotopes.

Before the activation the xenon sample was measured in the cavity for 26.5 days and the copper sample for 34.3 days. The pre-activation spectra were used to estimate the detection sensitivity to the γ-lines of the expected activation products as function of measuring time. The activation took place at 3450 m above the sea level, corresponding to an atmospheric depth of $728\,\mathrm{g/cm^2}$, where the CR flux is 11.2 times higher with respect to the sea level. After the activation the samples were stored for 4 days at an altitude of 795 m at Lauterbrunnen, where the CR flux was 2.4 time lower than the previous location and the activation took place at a reduced rate. The considered cool-down time of the activated samples, from the time they were brought underground until the start of the measurement, was 2.5 days for the xenon and 14.8 for the copper. The γ-spectrum was acquired over 11.5 days for the xenon and 4.0 days for the copper.

The intrinsic activity from a radioisotope is inferred from the intensity of its most prominent γ-lines in the post-activation spectrum. In order to infer the activity of a radioisotope from several of its γ-lines at the same time the spectrum was analysed with a Bayesian method, described in [37–39]. The spectrum around each line is divided in three regions, a central signal region and two lateral control regions. The signal region is defined as the $\pm 3\sigma$ around the mean position of the peak, where σ is the energy-dependent resolution determined by proper calibrations of the spectrometer [36]. The background in the signal region is inferred interpolating the counting rates in the control regions, 3σ above and below the signal region. Hence the total counting rate expected in the signal region is given by:

$$\gamma_{\mathrm{S}} = m \cdot A \cdot (\varepsilon \cdot \mathrm{BR}) + w_{\mathrm{S}} \frac{\beta_{\mathrm{L}} + \beta_{\mathrm{R}}}{w_{\mathrm{L}} + w_{\mathrm{R}}}, \tag{1}$$

where m is the sample mass, A is the specific activity of the sample, $\beta_{\mathrm{L,R}}$ are the background rates in the left and right control regions, respectively, and $w_{\mathrm{S,L,R}}$ are the widths of the three regions. The product of branching ratio BR and detection efficiency ε of the γ-line is calculated with Monte Carlo simulations, based on a detailed implementation of the detector and sample geometry in GEANT4 [40]. The decays of the radio-isotopes are simulated using the G4RadioactiveDecay class, where branching ratios and directional correlations are taken into account.

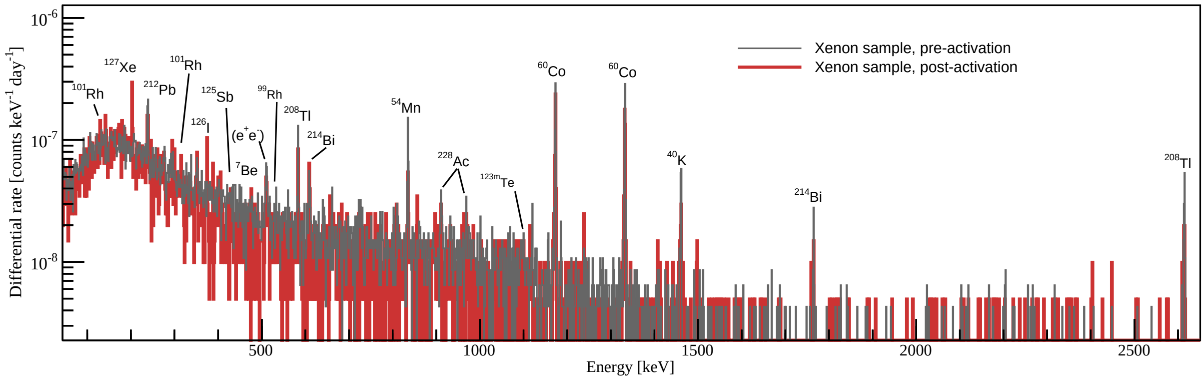

Figure 1. Pre- and post-activation spectra of the 2.04 kg xenon sample. One can identify the ^{127}Xe lines at 202.9 and 375.0 keV, and the ^{126}I line at 388.6 keV. Other prominent lines are from radioactive contaminations in the stainless steel bottle containing the xenon (primordial ^{238}U and ^{232}Th chains, ^{40}K, cosmogenic ^{54}Mn, ^{60}Co). Figure taken from [26].

Considering N γ-lines for the same isotope, the likelihood of the model is

$$\mathcal{L} = \prod_{k}^{N} f_P(C_{\mathrm{S}_k}|\gamma_{\mathrm{S}_k} t) \cdot f_P(C_{\mathrm{L}_k}|\beta_{\mathrm{L}_k} t) \cdot f_P(C_{\mathrm{R}_k}|\beta_{\mathrm{R}_k} t), \tag{2}$$

where the $C_{\mathrm{S}_k,\mathrm{L}_k,\mathrm{R}_k}$ are the counts in the three regions for each line k, and t is the measurement time. $f_P(C|\mu) = \mu^C/C!\ e^{-\mu}$ is the Poisson distribution.

The marginalized posterior probability density function (PDF) of the specific activity A is generated by Markov Chain Monte Carlo methods implemented in the Bayesian Analysis Toolkit (BAT) [41], where we use flat priors for the parameters γ_k and $\beta_{\mathrm{L}_k,\mathrm{R}_k}$. In Figure 2 some examples of marginalized posterior PDFs are shown for three different isotopes.

Since for some of the investigated isotopes the life time is comparable to the acquisition time, the specific activity A in Eq. 1 represents a mean specific activity over the measuring time. Hence the activity at the start of the acquisition, A_0 is:

$$A_0 = A \cdot \left(\frac{t}{\tau}\right)\left(1 - e^{-t/\tau}\right)^{-1}, \tag{3}$$

where τ is the radioisotope mean lifetime and t is the measurement time.
The specific activity of a sample of mass m after an activation time t is:

$$A(t) = \frac{N(t)}{m\ \tau} = P\left(1 - e^{-t/\tau}\right), \tag{4}$$

where P is the production rate which corresponds to the saturation activity $A(t \to \infty)$. Hence the production rate at the Jungfraujoch A_J is:

$$A_\mathrm{J} = A_0 e^{\left(\frac{t_\mathrm{c}+t_\mathrm{t}}{\tau}\right)} \left[\left(1 - e^{-t_\mathrm{a}/\tau}\right) + r\left(e^{t_\mathrm{t}/\tau} - 1\right)\right]^{-1}, \tag{5}$$

where t_a is the activation time at 3450 m, t_t is the activation time at 795 m, t_c is the cool-down time, and $r = P_\mathrm{t}/P_\mathrm{J}$ is the ratio of the production rates at Lauterbrunnen and Jungfraujoch, respectively.

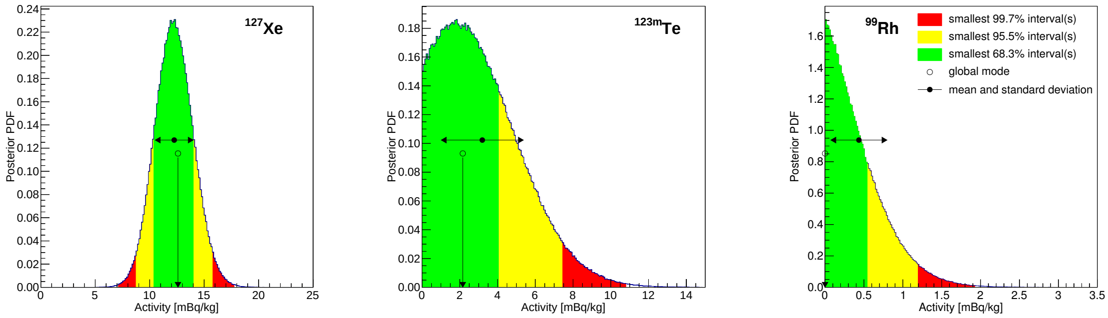

(a) (b) (c)

Figure 2. (a) Posterior PDF for the detected ^{127}Xe activity, clearly visible in Figure 1. The green region represents the shortest 68.3% C.I., which is taken as $\pm 1\,\sigma$ uncertainty. (b) For $^{123\mathrm{m}}$Te a signal is present, but an upper limit is reported since the intensity is too low to be determined. (c) An upper limit is reported for the activity of ^{99}Rh. The right edge of the yellow region represents the 95.5% upper limit (or the lower 95.5% C.I.). Figures extracted from [26].

3. Results and discussion

All the cosmogenic products of Cu that we identified are well known: they are spallation and fragmentation products of ^{63}Cu and ^{65}Cu, the only stable isotopes of copper. Most of these measurements (Table 2) are predicted within the 68 % credibility interval (CI) from the calculations performed with ACTIVIA and COSMO. The only exceptions are the measured activities of ^{57}Co and ^{58}Co that resulted $\sim 35\,\%$ and $\sim 20\,\%$ higher, respectively, with respect to the predictions. Furthermore five out of eight detected radioisotopes were found in agreement with the only other measurement available in literature so far, which was performed at LNGS [42] in 2009. In particular we observed production rates for ^{54}Mn, ^{57}Co and ^{60}Co lower by (2.5 ± 0.6), (1.7 ± 0.5) and (2.9 ± 0.8) times, respectively.

For the xenon sample we detected 5 cosmogenic products: ^{7}Be, ^{101}Rh, ^{125}Sb, ^{126}I and ^{127}Xe. The measured saturation activities are compared with the predictions with ACTIVIA and COSMO in Table 2. With the exception of ^{126}I, we observed a systematic underestimation of the production rates from the calculations performed with both packages. The observed production rate for ^{127}Xe was found in agreement within the 1σ CI with the measurement of the first 90 days of data reported by the LUX experiment ($1530 \pm 300\,\mu$Bq/kg) [43].

Among this detected radioactive products of xenon only the ^{101}Rh, ^{125}Sb have life times long enough to affect the sensitivity of an experiment foreseen to run for ~ 5 years. We point out that both elements have a relatively high electronegativity and might be reduced by the xenon purification systems, based on hot zirconium getters, and commonly used in LXe detectors. However, this has not yet been proved experimentally.

The ^{101}Rh decays by electron capture to one of the excited states of the ^{101}Ru, which deexcite emitting only low energetic γ-rays in rapid sequence (< 1 ns). This mechanism shifts, by pileup in LXe, the initial low energy recoils of the γ-rays to energies above the usual dark matter searching range.

On the other hand for the ^{125}Sb the situation is different as this isotope decays to ^{125}Te by β emission. In about 13.6 % of the decays the final state is the long-lived ($T_{1/2} = 57.4$ d) metastable state at 145 keV, without any sbsequent γ-ray. Hence the low energy tail of these β decays would produce single-scatter electronic recoil background in the dark matter searching region, while all the other decay paths will not contribute to the background in the same energy region.

Table 2. Selected results, extracted from [26], for the cosmogenic activation of OFCH copper and natural xenon. The specific saturation activities at sea level are compared to our predictions based on Activia and Cosmo. The half-lifes refer to the numbers used in the software packages.

Specific saturation activity at sea level A_{sat} [μBq/kg]

Copper					Xenon				
Isotope	$T_{1/2}$ [days]	Measurement	Calculations Activia	Cosmo	Isotope	$T_{1/2}$ [days]	Measurement	Calculation Activia	Cosmo
^{46}Sc	83.79	27^{+11}_{-9}	36	17	^{7}Be	53.3	370^{+240}_{-230}	6.4	6.4
^{48}V	15.97	39^{+19}_{-15}	34	36	^{101}Rh	1205.3	1420^{+970}_{-850}	16.6	15.3
^{54}Mn	312.12	154^{+35}_{-34}	166	156	^{125}Sb	986.0	590^{+260}_{-230}	0.2	13.5
^{59}Fe	44.50	47^{+16}_{-14}	49	50	^{126}I	13.0	175^{+94}_{-87}	247	247
^{56}Co	77.24	108^{+14}_{-16}	101	81	^{127}Xe	36.4	1870^{+290}_{-270}	415	555
^{57}Co	271.74	519^{+100}_{-95}	376	350					
^{58}Co	70.86	798^{+62}_{-58}	656	632					
^{60}Co	1925.28	340^{+82}_{-68}	304	297					

4. Conclusions

We performed the first dedicated experimental study of the cosmogenic activation of xenon, employed as detection medium, and the second dedicated measurement of cosmogenic activation of OFHC copper, often used for the internal parts of low background experiments.

The agreement of the production rates measured for copper with the calculations performed with ACTIVIA and COSMO packages, supports the validity of the cosmic rays model we employed for the xenon study. However the very poor agreement of the calculations performed by the same packages for xenon suggests that experimental studies of the production cross sections are required in order to get reliable predictions for the cosmogenic activation of this material. Among the five cosmogenic products detected in xenon only ^{125}Sb might constitute a problem for the next generation dark matter detectors, while we did not observe any radionuclide that could be a problem for experiments looking for $0\nu\beta\beta$ decays of ^{136}Xe. However considering the electronic background published by the LUX experiment and using the activation times quoted for their xenon [43] the production rate we measured for ^{125}Sb seems to be too high. Thus we conclude that the activation rate is either close to the lower end of our quoted credibility interval, or ^{125}Sb is removed by the xenon purification system or by plating-out at the surfaces.

The only detected inert noble gas isotope, which may pose a problem for the next multi-ton scale detectors for WIMP searches, is the ^{127}Xe. However, given its relatively short half life ($T_{1/2} = 36.3\,\text{d}$) the contamination from this isotope will be reduced already by an order of magnitude just after few months of storage underground.

As final remark we note that for the foreseen multi-ton scale LXe detectors, such as XENONnT [10], LZ [11] and DARWIN [5, 44], also the cosmogenic activation from the high energy muons fluxes in underground laboratories should be studied, as in this case the production in situ of short lived isotopes may contribute to the intrinsic background.

Acknowledgments

We gratefully acknowledge support from the staff and the International Foundation High Altitude Research Stations Jungfraujoch and Gornergrat (HFSJG) operating the Jungfraujoch laboratory [27], where the activation with cosmic rays was performed, the SNF grants 200020-149256 and 20AS21-136660, the ITN Invisibles (Marie Curie Actions, PITN-GA-2011-289442), Dr. D. Coderre, L. Bütikofer, and Dr. A.D. Ferella for help with transportation and handling the samples at LNGS, and Prof. Dr. C.J. Martoff for discussions on cosmogenic activation.

References

[1] Aprile E *et al.* (XENON Collaboration) 2012 *Astropart. Phys.* **35** 573
[2] Abe K *et al.* (XMASS Collaboration) 2013 *Nucl. Instr. Meth.* A **716** 78
[3] Akerib D S *et al.* (LUX Collaboration) 2013 *Nucl. Instr. Meth.* A **704** 111
[4] Aprile E *et al.* (XENON Collaboration) 2013, *Sources and Detection of Dark Matter and Dark Energy in the Universe. Proc. Symp. 10th UCLA DM2012, February 22-24, 2012* (Berlin: Springer) **148** 136 (*arXiv:*1206.6288)
[5] Schumann M *et al.* 2015 *JCAP* **10** 016 (*arXiv:*1506.08309)
[6] Jungman G *et al.* 1996 *Phys. Rept.* **267** 195
[7] Bertone G 2005 *Phys. Rept.* **405** 279
[8] Plante G *et al.* 2011 *Phys. Rev.* C **84** 045805
[9] Manalaysay A *et al.* 2010 *Rev. Sci. Instr.* **81** 073303
[10] Aprile E*et al.* (XENON Collaboration) 2014 *JINST* **9** P11006
[11] Malling D C*et al.* (LZ Collaboration) 2011 (*arXiv:*1110.0103)
[12] Auger M *et al.* (EXO Collaboration) 2012 *Phys. Rev. Lett.* **109** 032505
[13] Gando A *et al.* (KamLAND-Zen Collaboration) 2012 *Phys. Rev.* C **85** 045504
[14] Gando A *et al.* (KamLAND-Zen Collaboration) 2013 *Phys. Rev. Lett.* **110** 062502
[15] Martin Albo J *et al.* (NEXT Collaboration) 2013 *J. Phys.: Conf. Ser.* **460** 012010
[16] Nuclear Structure and Decay Database (NuDat 2.6), `http://www.nndc.bnl.gov/nudat2/`
[17] Shukla A *et al.* 2007 *J. Phys.* G*: Nucl. Phys.* **34** 549
[18] Rosman K J R and Taylor P D P (IUPAC) 1998 *Pure and Appl. Chem.* **70** 217
[19] Back J J and Ramachers Y A 2008 *Nucl. Instr. Meth.* A **586** 286
[20] Martoff C J and Lewin P D 1992 *Comput. Phys. Comm.* **72** 96
[21] Aprile E *et al.* (XENON Collaboration) 2011 *Phys. Rev.* D **83** 082001
[22] Kish A 2011 *PhD thesis* University of Zurich (`http://opac.nebis.ch/ediss/20121322.pdf`)
[23] Silberberg R and Tsao C H 1973 *Astrophys. J. Suppl.* 220 (I) **25** 315
[24] Silberberg R and Tsao C H 1973 *Astrophys. J. Suppl.* 220 (II) **25** 335
[25] Silberberg R *et al.* 1998 *Astrophys. J.* **501** 911
[26] Baudis L *et al.* 2015 *EPJ* C **75** 485
[27] `http://www.ifjungo.ch/jungfraujoch/`
[28] Aprile E *et al.* (XENON Collaboration) 2011 *Astropart. Phys.* **35** 43
[29] Beatty J J *et al.* 2004 *Phys. Rev.* D **70** 092005
[30] Heisinger B *et al.* 2002 Earth and Planetary Sci. Lett. **200** 345
[31] Hagner T *et al.* 2000 *Astropart. Phys.* **14** 33
[32] Ziegler J F 1996 *J. Res. Develop* **40** 19
[33] Stanev T 2010 *High Energy Cosmic Rays, 2nd*, Chichester UK, Praxis Publishing Ltd
[34] Beringer J *et al.* (Particle Data Group) 2012 *Phys. Rev.* D **86** 010001
[35] U.S. Standard Atmosphere 1976, `http://www.pdas.com/atmos.html`
[36] Baudis L *et al.* 2011 *JINST* **6** P08010
[37] Weise K and Matzke M 1989 *Nucl. Instr. Meth.* A **280** 103
[38] Weise K and Woger W 1992 *Meas. Sci. Techn.* **3** 1
[39] Lira I and Grientschnig D 2010 *Metrologia* **47** R1
[40] Agostinelli S *et al.* (GEANT4) 2003 *Nucl. Instr. Meth.* A **506** 250
[41] Caldwell A *et al.* 2009 *Comp. Phys. Comm.* **180** 2197
[42] Laubenstein M and Heusser G 2009 *Appl. Rad. Isot.* **67** 750
[43] Akerib D S *et al.* (LUX Collaboration) 2015 *Astropart. Phys.* **62** 33
[44] Baudis L *et al.* 2014 *JCAP* **01** 044